

MoM/BI-RME Analysis of Boxed MMICs with Arbitrarily Shaped Metallizations

Maurizio Bozzi, *Member, IEEE*, Luca Perregrini, *Member, IEEE*,
Alejandro Alvarez Melcón, *Member, IEEE*, Marco Guglielmi, *Senior Member, IEEE*, and
Giuseppe Conciauro, *Member, IEEE*

Abstract—In this paper, we propose a novel approach for the analysis of shielded microstrip circuits, composed of a number of thin metallic areas with arbitrary shapes and finite conductivity, embedded in a multilayered lossy medium. The analysis is based on the solution of an Integral Equation (IE) obtained by enforcing the proper boundary condition to the electric field on the metallic areas. The solution of the IE is obtained by the Method of Moments (MoM) with entire domain basis functions, which are numerically determined by the Boundary Integral-Resonant Mode Expansion (BI-RME) method. The use of the BI-RME method allows for the efficient calculation of the basis functions independently on the shape of the domain, thus permitting the analysis of a wide class of circuits. Two examples demonstrate the accuracy, rapidity, and flexibility of the proposed method.

Keywords—MMICs, Integral Equations, Moment Method, Entire Domain Basis Functions, Microstrip Filters.

I. INTRODUCTION

In the last years, a considerable interest has been directed to the design of boxed multilayered circuits (Fig. 1). This configuration is typically considered in the design of many actual Monolithic Microwave Integrated Circuits (MMICs), both in single-layer [1] and in multilayered configuration [2,3].

Among the possible numerical methods applied to the analysis of this type of structures, the Integral Equation (IE) method is by far one of the most efficient. The IE method can be formulated either in the spectral [4] or in the spatial domain [5]. The resulting integral equation is solved by the Method of Moments (MoM), usually considering sub-domain basis functions (*e.g.*, roof-tops [6,7] or basis functions on triangular domains [8,9]).

Recently, the IE/MoM method in the spectral domain was applied with entire domain basis functions [10]. The main advantage of using the vector modal functions derived in that work is the dramatic reduction in the order of the MoM matrix, since few entire domain basis functions are usually sufficient to represent the unknown currents.

Manuscript received ...; revised ...

This work was supported by the European Commission under project MMCODEF, contract No. HPRN-2000-00043, and by Consiglio Nazionale delle Ricerche (CNR) under contract MADESS II.

M. Bozzi, L. Perregrini and G. Conciauro are with the Department of Electronics of the University of Pavia, Via Ferrata 1, 27100 Pavia, Italy. E-mail: maurizio.bozzi@ele.unipv.it, luca.perregrini@ele.unipv.it, giuseppe.conciauro@ele.unipv.it.

A. Alvarez Melcón is with the Technical University of Carthagene, Campus Muralla del Mar s/n, 30202 Cartagena, Spain.

E-mail: alejandro.alvarez@upct.es.

M. Guglielmi is with the European Space Research and Technology Center, ESA-ESTEC, 2200AG Noordwijk, The Netherlands. E-mail: marco.guglielmi@esa.int.

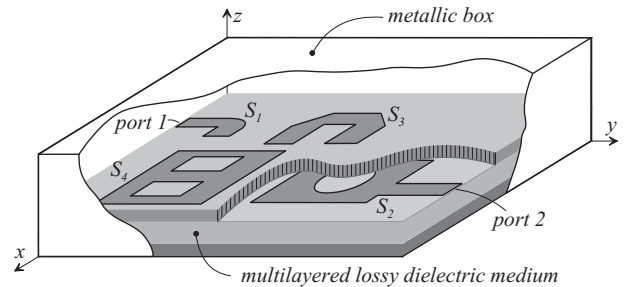


Fig. 1. A shielded MMIC with arbitrarily shaped metallic areas in a multilayered lossy medium. The patches can be placed at different height and they may overlap.

Moreover, the calculation of the MoM matrix is enhanced because of the rapid decrease of the spectral components to be added subsequently for the calculation of the matrix elements. It is noted, however, that the original work derived in [10] is limited to areas with a rectangular shape, where the entire domain basis functions are known analytically.

In this paper, we present the extension of the method proposed in [10] to the case of metallic areas with an arbitrary shape (Fig. 1). The entire domain basis functions are determined numerically by the Boundary Integral-Resonant Mode Expansion (BI-RME) method [11]. The use of the BI-RME method has two main advantages. The first is the possibility of obtaining entire domain basis functions for arbitrary shapes in a short time, and the second is that the entries of the MoM matrix are practically obtained as a by-product of the method itself. In fact, the surface integrals involved in the calculations of the MoM matrix can be converted into line integrals on the boundary of the metallic areas, and the quantities required on the boundary are the basic output of the BI-RME calculation.

A preliminary discussion of the proposed algorithm was presented in [12]. This paper gives a comprehensive explanation of the MoM/BI-RME method, adding two novel capabilities: metallic areas including a port may have an arbitrary shape, and multiply connected metallizations can be considered.

II. IE/MOM APPROACH

Let us consider the structure shown in Fig. 2, consisting of a multilayered medium and P metallic areas with arbitrary shapes S_1, \dots, S_P , possibly located at different interfaces. The circuit is fed at the frequency ω at K ports, ($K \leq P$) conventionally defined on the first K areas S_1, \dots, S_K .

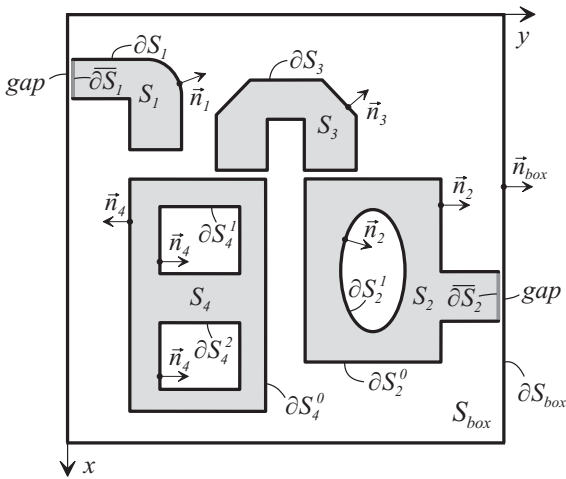


Fig. 2. Different metallic areas considered in the analysis: simply (S_1) or multiply connected patches attached to a port (S_2), simply (S_3) or multiply connected internal patches (S_4). ∂S_p represents the boundary of the area S_p except the possible part corresponding to a port (denoted by $\overline{\partial S_p}$). In case of multiply connected areas, ∂S_p consists of many lines $\partial S_p^0, \partial S_p^1, \dots$

As usual [5,13,14], the ports are represented as small gaps between the metallization and the wall of the box (delta-gap excitations).

In [10] the analysis is based on the solution of a system of P integral equations, which are obtained by enforcing the boundary condition to the transverse-to- z electric field at all the metallic areas:

$$\begin{aligned} Z \vec{J}_p(\vec{r}) - \sum_{q=1}^P \int_{S_q} \overleftrightarrow{G}(\vec{r}, \vec{r}' | \omega) \cdot \vec{J}_q(\vec{r}') dS' = \\ = \begin{cases} -\vec{n}_p v_p \delta(\vec{r}, \vec{r}') |_{\vec{r}' \in \overline{\partial S_p}} & (p = 1, \dots, K) \\ 0 & (p = K + 1, \dots, P) \end{cases} \quad (1) \end{aligned}$$

where: the points \vec{r}, \vec{r}' belongs to S_p and S_q , respectively; $\overline{\partial S_p}$ denotes the part of the boundary of S_p that belongs to the p -th port; \vec{n}_p is the outward normal; v_p is the voltage applied to the p -th port; Z is the “sheet impedance” of the metallizations. The choice of Z is problem-dependent. For instance: in the case of a single-layer microstrip circuit with a metallization thickness t much larger than the skin depth δ , we can use the surface impedance of the conductors $Z = Z_s = (1 + j)\rho/\delta$ (ρ is the resistivity of the metal); in the case of low frequency calculations ($t \ll \delta$), we can use $Z = \rho/t$. Moreover, \vec{J}_q is the (unknown) current density on S_q , and the Green’s function \overleftrightarrow{G} is given by [15]

$$\overleftrightarrow{G}(\vec{r}, \vec{r}' | \omega) = \sum_m V_m(z, z' | \omega) \vec{\mathcal{E}}_m(x, y) \vec{\mathcal{E}}_m(x', y') \quad (2)$$

where $\vec{\mathcal{E}}_m$ are the transverse electric modal vectors of the TE and TM modes of the box, with the normalization $\int_{S_{box}} |\vec{\mathcal{E}}_m|^2 dS = 1$. The expressions of $\vec{\mathcal{E}}_m$ are

$$\vec{\mathcal{E}}_m' = -\frac{\nabla_T \chi_m'}{k_m'} \quad (\text{TM modes}) \quad (3)$$

$$\vec{\mathcal{E}}_m'' = -\vec{u}_z \times \frac{\nabla_T \chi_m''}{k_m''} \quad (\text{TE modes}) \quad (4)$$

where χ_m' and χ_m'' are the eigenfunctions of the Helmholtz equation with the Dirichlet or Neumann boundary conditions on ∂S_{box} (see Fig. 2), and k_m', k_m'' are the corresponding eigenvalues. Finally, functions V_m are determined by considering the equivalent modal transmission lines for the layered box [10,16].

Equation (1) is solved by applying the MoM in the Galerkin version. The unknown current density \vec{J}_p is represented through a suitable set of N_p basis functions $\vec{e}_r^{(p)}$ defined on the p -th patch

$$\vec{J}_p = \sum_{r=1}^{N_p} \xi_r^{(p)} \vec{e}_r^{(p)} \quad (p = 1, \dots, P) \quad (5)$$

where $\xi_r^{(p)}$ are unknown coefficients.

As discussed in [10], the calculation of the MoM matrices involves frequency-independent coefficients of two types. The former represents the *coupling integral* between the r -th basis function on the p -th metallic area and the m -th modal vector of the box, and is given by

$$\mathcal{C}_{rm}^{(p)} = \int_{S_p} \vec{e}_r^{(p)}(\vec{r}) \cdot \vec{\mathcal{E}}_m(\vec{r}) dS \quad (6)$$

The latter is the projection of the delta-gap excitation of the p -th port on the r -th basis function (*port integral*), and is given by

$$\mathcal{P}_r^{(p)} = \int_{\overline{\partial S_p}} \vec{e}_r^{(p)}(\vec{r}) \cdot (-\vec{n}_p) dl \quad (7)$$

For any frequency, the scattering parameters are calculated straightforwardly from the coefficients $\xi_r^{(p)}$ obtained by the solution of the MoM system [10].

III. ENTIRE DOMAIN BASIS FUNCTIONS

A key feature of the present approach is the use of a set of entire domain basis functions, *i.e.*, functions $\vec{e}_r^{(p)}$ which span the entire domain S_p .

The advantage of using such functions has been demonstrated in [10], with reference to the case where all surfaces S_p are rectangular. More specifically, the electric modal vectors of rectangular waveguides bounded by magnetic or mixed-type walls have been used as basis functions. In this paper the same concept is applied to metallization of arbitrary shapes, with no restriction on the geometry of the surfaces S_p . In this case, the basis functions must be determined numerically and the efficiency of the numerical method used for their calculation is a vital issue. The BI-RME method discussed in Sec. V permits to determine very efficiently a lot of basis functions.

In the case of simply connected surfaces, we have to calculate two classes of basis functions expressed by

$$\vec{e}_r^{(p)} = -\vec{u}_z \times \frac{\nabla_T \psi_r^{(p)}}{\kappa_r^{(p)}} \quad (8)$$

$$\vec{e}_r^{(p)} = -\frac{\nabla_T \psi_r^{(p)}}{\kappa_r^{(p)}} \quad (9)$$

where the pairs $\{\psi_r^{(p)}, \kappa_r^{(p)}\}$ and $\{\psi_r^{(p)}, \kappa_r^{(p)}\}$ are the eigensolutions of the homogeneous Helmholtz equation in the domain S_p , i.e.,

$$\nabla_T^2 \psi_r^{(p)} + \kappa_r^{(p)2} \psi_r^{(p)} = 0 \quad \text{in } S_p \quad (10)$$

$$\nabla_T^2 \psi_r^{(p)} + \kappa_r^{(p)2} \psi_r^{(p)} = 0 \quad \text{in } S_p \quad (11)$$

In the case of N -times connected surfaces, the set of basis functions must be supplemented with $N - 1$ additional functions

$$\vec{e}_r^{0(p)} = -\vec{u}_z \times \nabla_T \psi_r^{0(p)} \quad (12)$$

where $\psi_r^{0(p)}$ satisfy the Laplace equation in the domain S_p , i.e.,

$$\nabla_T^2 \psi_r^{0(p)} = 0 \quad \text{in } S_p \quad (13)$$

The boundary conditions are different for metallizations connected or not connected to ports.

In the case of metallizations not connected to ports (*e.g.*, S_3 and S_4 in Fig. 2), \vec{J}_p is tangent to the whole boundary of S_p . The same boundary condition on the basis functions is satisfied provided that

$$\psi_r^{(p)} = 0 \quad \text{on } \partial S_p \quad (14)$$

$$\partial \psi_r^{(p)} / \partial n_p = 0 \quad \text{on } \partial S_p \quad (15)$$

$$\psi_r^{0(p)} = \begin{cases} 1 & \text{on the inner contour } \partial S_p^i \\ 0 & \text{on } \partial S_p - \partial S_p^i \end{cases} \quad (16)$$

In the case of metallizations connected to ports (*e.g.*, S_1 and S_2 in Fig. 2), \vec{J}_q is perpendicular to the port segment $\overline{\partial S_p}$. In this case, $\psi_r^{(p)}$, $\psi_r^{(p)}$, and $\psi_r^{0(p)}$ must satisfy the mixed boundary conditions

$$\begin{cases} \psi_r^{(p)} = 0 & \text{on } \partial S_p \\ \partial \psi_r^{(p)} / \partial n_p = 0 & \text{on } \overline{\partial S_p} \end{cases} \quad (17)$$

$$\begin{cases} \partial \psi_r^{(p)} / \partial n_p = 0 & \text{on } \partial S_p \\ \psi_r^{(p)} = 0 & \text{on } \overline{\partial S_p} \end{cases} \quad (18)$$

$$\begin{cases} \psi_r^{0(p)} = \begin{cases} 1 & \text{on the inner contour } \partial S_p^i \\ 0 & \text{on } \partial S_p - \partial S_p^i \end{cases} \\ \partial \psi_r^{0(p)} / \partial n_p = 0 & \text{on } \overline{\partial S_p} \end{cases} \quad (19)$$

It is worthy noting that, in the case of metallizations connected to ports, ∂S_p denotes the boundary of S_p but the port segment $\overline{\partial S_p}$.

IV. COUPLING AND PORT INTEGRALS

When considering metallic areas with a rectangular shape the coupling integrals (6) and the port integrals (7) can be calculated analytically by using the analytical expressions of the basis functions (see [10], for instance). This possibility is precluded in the case of arbitrary shapes, because the basis functions are determined numerically. In this case, the surface integration (6) is a time consuming task, especially in cases of basis functions determined by a boundary integral method, since it requires the numerical evaluation of the basis functions in many points within the integration domain S_p . However, the coupling integrals (6) can be transformed from surface to line integrals, thus reducing dramatically the computing time. As shown in the Appendix, we have

$$\int_{S_p} \vec{e}_r^{(p)} \cdot \vec{\mathcal{E}}_m^l dS = 0 \quad (20)$$

$$\int_{S_p} \vec{e}_r^{(p)} \cdot \vec{\mathcal{E}}_m^l dS = \frac{\kappa_r^{(p)}}{k_m'(\kappa_r^{(p)2} - k_m'^2)} \int_{\partial S_p} \psi_r^{(p)} \frac{\partial \chi_m'}{\partial n_p} dl \quad (21)$$

$$\int_{S_p} \vec{e}_r^{0(p)} \cdot \vec{\mathcal{E}}_m^l dS = 0 \quad (22)$$

$$\int_{S_p} \vec{e}_r^{(p)} \cdot \vec{\mathcal{E}}_m'' dS = \frac{k_m''}{\kappa_r^{(p)}(\kappa_r^{(p)2} - k_m''^2)} \int_{\partial S_p} \chi_m'' \frac{\partial \psi_r^{(p)}}{\partial n_p} dl \quad (23)$$

$$\int_{S_p} \vec{e}_r^{(p)} \cdot \vec{\mathcal{E}}_m'' dS = \frac{1}{\kappa_r^{(p)} k_m''} \int_{\partial S_p} \psi_r^{(p)} \frac{\partial \chi_m''}{\partial t_p} dl \quad (24)$$

$$\int_{S_p} \vec{e}_r^{0(p)} \cdot \vec{\mathcal{E}}_m'' dS = -\frac{1}{k_m''} \int_{\partial S_p} \chi_m'' \frac{\partial \psi_r^{0(p)}}{\partial n_p} dl \quad (25)$$

where $\partial/\partial t_p$ is the derivative along the boundary, namely in the direction of $\vec{t}_p = \vec{u}_z \times \vec{n}_p$.

It is noted that these formulas hold true in both cases of metallizations connected or not connected to ports.

For the port integrals (7), we easily obtain

$$\int_{\overline{\partial S_p}} \vec{e}_r^{(p)}(\vec{r}) \cdot (-\vec{n}_p) dl = 0 \quad (26)$$

$$\int_{\overline{\partial S_p}} \vec{e}_r^{(p)}(\vec{r}) \cdot (-\vec{n}_p) dl = \frac{1}{\kappa_r^{(p)}} \int_{\overline{\partial S_p}} \frac{\partial \psi_r^{(p)}}{\partial n_p} dl \quad (27)$$

$$\int_{\overline{\partial S_p}} \vec{e}_r^{0(p)}(\vec{r}) \cdot (-\vec{n}_p) dl = 0 \quad (28)$$

V. APPLICATION OF THE BI-RME METHOD

In the analysis of circuits of practical interest some tens of basis functions (8) and (9) are usually needed for each metallic area. This, in turn, requires the calculation of some tens of eigensolutions of the Helmholtz equations (10), (11).

In the past years, some of the authors developed a novel method (the BI-RME method) for the solution of the Helmholtz equation in arbitrary domains [17,18,19]. A comprehensive description of the BI-RME method is reported in

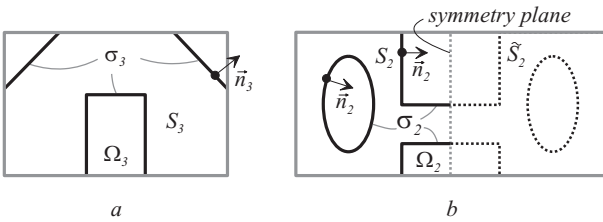


Fig. 3. Geometry for the application of the BI-RME method: a) an internal metallic area, b) a metallic area connected to a port.

a book [11]. In this section, we limit ourselves to a brief outline of the BI-RME method, to highlight its advantages in the calculation of entire domain basis functions.

The BI-RME method is a modified boundary integral approach for the evaluation of eigenfunctions. The surface S_p (either simply or multiply connected) is considered as a part of a fictitious enlarged domain Ω_p with a rectangular shape (Fig. 3a). The eigenfunctions to be determined are defined in Ω_p , and are assumed to vanish outside S_p . They are expressed as combinations of Boundary Integrals (BI) and a Resonant Mode Expansion (RME), involving the modal potentials of the region Ω_p . The boundary integrals involve $\partial\psi_r^{(p)}/\partial n_p$ and $\psi_r^{(p)}$ over the line σ_p (see Fig. 3a), which corresponds to the part of ∂S_p not coincident with the rectangular boundary. Using the BI-RME representation of the eigenfunctions and imposing the proper boundary conditions on σ_p , the eigenvalue problems (10) and (11) are converted into integral-differential equations. As in the case of the conventional Boundary Element Method (BEM), the discretized problem resulting from the application of the BI-RME method is much smaller than in conventional approaches based on differential equations (FEM, FDFD, ...). Differently from the conventional BEM, the BI-RME method leads to the determination of the eigenfunctions by the solution of a linear matrix eigenvalue problem. In particular, it provides as eigenvalues $\kappa_r^{(p)}$ and $\kappa_r^{(p)}$ up to a prescribed value κ_{max} , and as eigenfunctions $\partial\psi_r^{(p)}/\partial n_p$ and $\psi_r^{(p)}$ over the line σ_p and the modal amplitudes of the RME.

The method is very efficient and reliable, also in cases where a large number of eigenfunctions have to be determined. Moreover, no spurious modes are found. Furthermore, it is worth noting that the order of the matrix eigenvalue problem to be solved depends on the extension of the line σ_p and the surface of the resonator Ω_p . For this reason, the efficiency of the BI-RME method highly improves when a large part of the boundary of S_p fits with the rectangular boundary as in the example in Fig. 3a.

The evaluation of coupling integrals (21), (23), and (24) requires $\partial\psi_r^{(p)}/\partial n_p$ and $\psi_r^{(p)}$ on ∂S_p . On the portion σ_p , these quantities are directly the solutions of the BI-RME method. On the other part of ∂S_p , they are obtained from the BI-RME representation of the eigenfunctions (see (5.44) and (5.94) in [11].) Even if a post-processing is required for obtaining the boundary values on $\partial S_p - \sigma_p$, it is convenient to let ∂S_p coincide with $\partial\Omega_p$ as much as possi-

ble. In fact, this reduces the dimensions of the eigenvalue problems to be solved, thus increasing the rapidity and accuracy of the solution.

To solve the Helmholtz equation in the case of a metallization connected to a port, the exterior domain Ω_p includes not only S_p , but also its mirror image \tilde{S}_p , as shown in Fig. 3b. The problem is solved by imposing an even or an odd symmetry condition with respect to the symmetry plane shown in Fig. 3b. The details on the implementation of the BI-RME method taking into account the symmetries are discussed in [11], Sec. 5.2.3.

Finally, for multiply connected surfaces, all the possible basis functions (12) must be considered, requiring the determination of all the solutions $\psi_r^{(p)}$ of the Laplace equation (13). These basis functions are obtained by solving (13) through the conventional BEM [17]. Even in this case, when the patch is connected to a port it is possible to solve the Laplace equation by creating a mirror image \tilde{S}_p of S_p , and considering an even symmetry condition on the symmetry plane.

VI. NUMERICAL RESULTS

We used the code for the analysis of printed circuits involving resonators with complex shapes, which fully exploit the capabilities of the method.

The first example refers to the analysis of a narrow-band microstrip filter composed of two T-shaped port elements and two square-loop resonators (Fig. 4), firstly proposed in [20]. The results obtained by the MoM/BI-RME approach are reported in Fig. 5 and compared with experimental data and simulations given in [20], showing a good agreement. The convergence was obtained with 4000 modes of the box and 62 basis functions (8 on each T-shaped line and 23 on each loop resonator), corresponding to $\kappa_{max} = 1.153 \text{ mm}^{-1}$.

For this example, we report in Fig. 6 the study of the convergence properties of the MoM/BI-RME method. In particular, we verified the convergence when varying the number of basis functions (Fig. 4a), and when varying the number of modes of the box (Fig. 4b). These graphs show that the frequency response does not change when considering more than 62 basis functions or more than 4000 modes of the box.

The calculation of the frequency response of Fig. 4 takes 22 sec for the determination of the basis functions and the evaluation of the coupling and port integrals, and 0.135 sec for the MoM solution in each frequency point (on a Pentium III at 1 GHz). Thus, the total computing time for the analysis in 100 frequency points is 35.5 sec. It is worthy observing that taking advantage of the symmetries of the geometry (which were not exploited in our analysis) should lead to a dramatic reduction of the total computing time.

The second example refers to the analysis of a narrow-band microstrip filter composed of two open-loop resonators (Fig. 7) [20]. The analysis of this structure (already presented in [12]) is particularly challenging, since the lines and the loops are separated by very narrow capacitive gaps, and the surface current must be accurately

represented near these gaps. Consequently, in this case, the analysis requires more basis functions than in the previous example. Fig. 8 shows the frequency response of the filter considering 4000 modes of the box and 158 basis functions (12 on each port line, 22 on the middle line, and 56 on each open-loop) corresponding to $\kappa_{max} = 3.144 \text{ mm}^{-1}$. The results are a good agreement with the theoretical and experimental data taken from [20]. The computing time (without exploiting the symmetries) is 48 *sec* for the calculation of the basis functions and of the coupling and port integrals, and 0.63 *sec* for the MoM solution in each frequency point (on a Pentium III at 1 GHz). Thus, the total computing time for the analysis in 100 frequency points is 111 *sec*.

As a final remark, we can observe that the selection of the basis functions in our approach is performed by a spectral criterion, including all the entire domain basis functions up to a prescribed κ_{max} . Especially in cases of metallizations where one of the dimensions is much larger than the other (*e.g.*, narrow strips), this criterion leads to the adoption of very large values of κ_{max} , in order to include in the set of basis functions a sufficient number of elements with significant variation along the narrow dimension. Of course, it can happen that many basis functions with uselessly rapid variation in the larger direction can be included in the basis. These functions could be discarded, but the procedure for their recognition is too complicate to be conveniently implemented in a general purpose computer code. Anyway, the numerical experiments presented above permit not to dramatize the problem, because we noted that it is sufficient to consider basis functions whose variation in the narrow dimension correspond to one or two sinusoidal oscillations. In spite of the roughness of the current representation the results are very good: this is, probably, dependent on the variational properties of the admittance parameters obtained by the Galerkin procedure.

VII. CONCLUSION

We have presented an efficient technique for the accurate analysis of multilayered shielded printed circuits composed of arbitrary shaped metallic areas. This technique is based on an Integral Equation solved by using the Method of Moments with entire domain basis functions. The basis functions are efficiently evaluated by the Boundary Integral-Resonant Mode Expansion method. This leads to MoM matrices of small size, even in the case of complex circuits. Moreover, the transformation of the coupling integrals from surface to line integrals permits to use the basic outputs of the BI-RME method for calculating the MoM matrix.

The analyses of circuits of practical interest have been reported and compared with both theoretical and experimental data, showing that the approach is indeed feasible and leads to a software code which is efficient and accurate.

APPENDIX

Following a procedure similar to the one presented in [21,22], the transformation of the coupling integrals from surface to line integrals is based on the application of

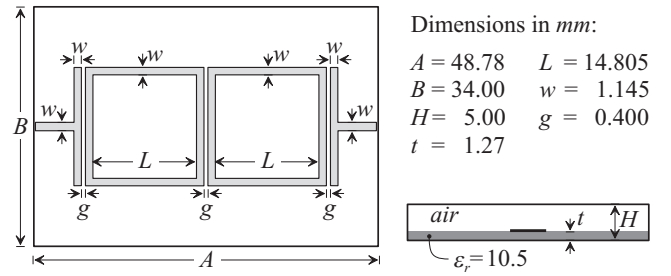


Fig. 4. Printed microstrip filter composed of T-shaped port elements and loop resonators.

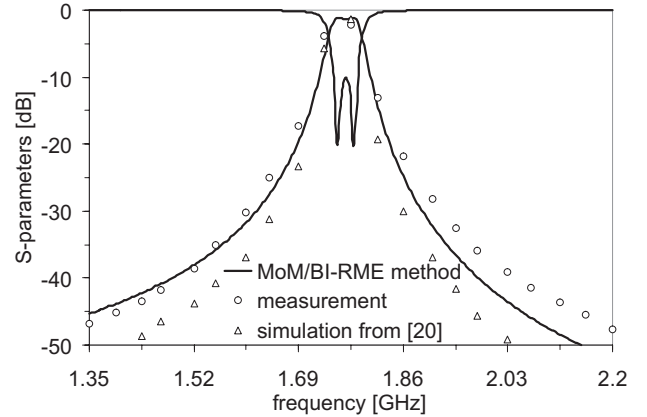


Fig. 5. Comparison between simulated and measured results presented in [20], and results obtained with the present approach, for the filter shown in Fig. 4.

Green's identity (see, for instance, [23], Appendix 2, Eq. 45)

$$\begin{aligned} \int_{S_p} \vec{A} \cdot \nabla_T \mathcal{B} dS &= \int_{\partial S_p} \mathcal{B} \vec{n} \cdot \vec{A} dl + \\ &+ \int_{\partial S_p} \mathcal{B} \vec{n} \cdot \vec{A} dl - \int_{S_p} \mathcal{B} \nabla_T \cdot \vec{A} dS \end{aligned} \quad (\text{A.1})$$

In the case of internal patches, obviously, the port segment ∂S_p is not defined and the line integral on ∂S_p vanishes.

Derivation of (20)

The electric modal fields are related to scalar potentials through (8) and (3), thus resulting

$$\begin{aligned} \int_{S_p} \vec{e}_r^{(p)} \cdot \vec{e}_m' dS &= \int_{S_p} \vec{u}_z \times \frac{\nabla_T \psi_r^{(p)}}{\kappa_r^{(p)}} \cdot \frac{\nabla_T \chi_m'}{k_m'} dS \\ &= -\frac{1}{\kappa_r^{(p)} k_m'} \int_{S_p} \nabla_T \psi_r^{(p)} \cdot \vec{u}_z \times \nabla_T \chi_m' dS \end{aligned} \quad (\text{A.2})$$

By applying (A.1) to (A.2) with $\vec{A} = \vec{u}_z \times \nabla_T \chi_m'$ and $\mathcal{B} = \psi_r^{(p)}$, we have

$$\begin{aligned} \int_{S_p} \vec{e}_r^{(p)} \cdot \vec{e}_m' dS &= -\frac{1}{\kappa_r^{(p)} k_m'} \int_{\partial S} \psi_q^{(p)} \vec{n}_p \cdot \vec{u}_z \times \nabla_T \chi_m' dl \\ &- \frac{1}{\kappa_r^{(p)} k_m'} \int_{\partial S_p} \psi_q^{(p)} \vec{n}_p \cdot \vec{u}_z \times \nabla_T \chi_m' dl \\ &+ \frac{1}{\kappa_r^{(p)} k_m'} \int_{S_p} \psi_r^{(p)} \nabla_T \cdot (\vec{u}_z \times \nabla_T \chi_m') dS \end{aligned} \quad (\text{A.3})$$

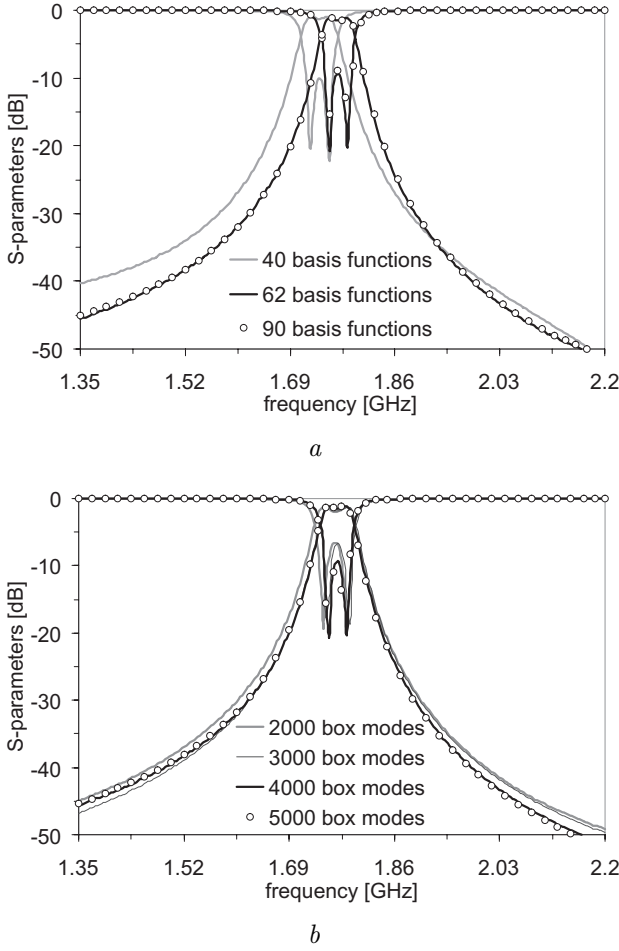


Fig. 6. Convergence behavior of the MoM/BI-RME method in the analysis of the circuit shown in Fig. 4: a) as a function of the total number of basis functions, when considering 4000 modes of the box; b) as a function of the number of modes of the box, when considering 62 basis functions.

In the r.h.s. of (A.3) the surface integral vanishes because of

$$\nabla_T \cdot (\vec{u}_z \times \nabla_T \mathcal{F}) = 0 \quad (\text{A.4})$$

for any scalar function \mathcal{F} (see, for instance, [23], Appendix 2, Eq. 38), whereas the line integral on ∂S_p vanishes since $\psi_r^{(p)} = 0$ on ∂S_p . Moreover, the line integral on $\overline{\partial S_p}$ is not defined for internal patches and, in the case of patches attached to ports, vanishes since $\vec{n}_p \cdot \vec{u}_z \times \nabla_T \chi'_m = -\partial \chi'_m / \partial t_p = 0$ on $\overline{\partial S_p}$. This proves (20).

Derivation of (21)

From (9) and (3) we have

$$\begin{aligned} \int_{S_p} \vec{e}_r^{(p)} \cdot \vec{\mathcal{E}}'_m dS &= \int_{S_p} \frac{\nabla_T \psi_r^{(p)}}{\kappa_r^{(p)}} \cdot \frac{\nabla_T \chi'_m}{k'_m} dS \\ &= \frac{1}{\kappa_r^{(p)} k'_m} \int_{S_p} \nabla_T \psi_r^{(p)} \cdot \nabla_T \chi'_m dS \end{aligned} \quad (\text{A.5})$$

By applying (A.1) to (A.5) with $\vec{\mathcal{A}} = \nabla_T \chi'_m$ and $\mathcal{B} = \psi_r^{(p)}$, and using the Helmholtz equation $\nabla_T^2 \chi'_m = -k_m'^2 \chi'_m$, we

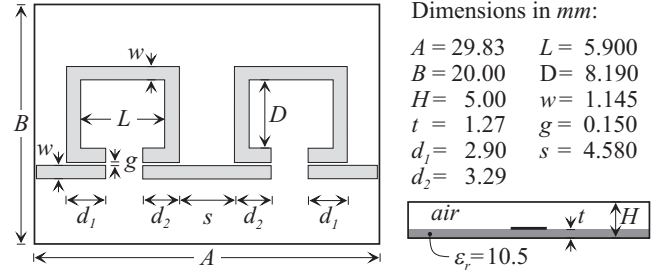


Fig. 7. Printed microstrip filter composed of two open-loop resonators.

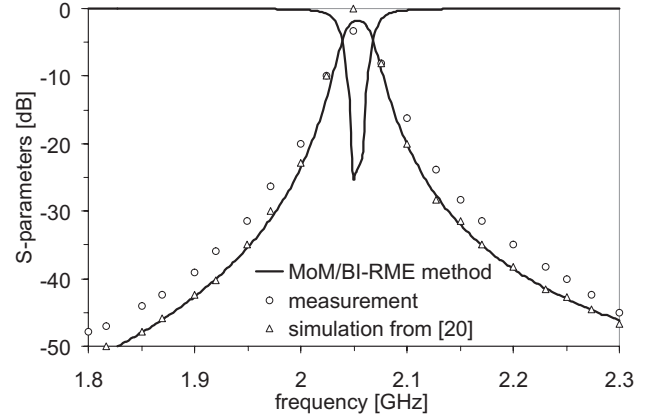


Fig. 8. Comparison between simulated and measured results presented in [21], and results obtained with the present approach, for the filter shown in Fig. 7.

have

$$\begin{aligned} \int_{S_p} \vec{e}_r^{(p)} \cdot \vec{\mathcal{E}}'_m dS &= \frac{1}{\kappa_r^{(p)} k'_m} \int_{\partial S_p} \psi_r^{(p)} \vec{n}_p \cdot \nabla_T \chi'_m dl \\ &+ \frac{1}{\kappa_r^{(p)} k'_m} \int_{\overline{\partial S_p}} \psi_r^{(p)} \vec{n}_p \cdot \nabla_T \chi'_m dl \\ &+ \frac{k'_m}{\kappa_r^{(p)}} \int_{S_p} \psi_r^{(p)} \chi'_m dS \end{aligned} \quad (\text{A.6})$$

By remembering that $\psi_r^{(p)} = 0$ on $\overline{\partial S_p}$, the line integral on $\overline{\partial S_p}$ in (A.6) vanishes.

Moreover, by applying (A.1) to (A.5) with $\vec{\mathcal{A}} = \nabla_T \psi_r^{(p)}$ and $\mathcal{B} = \chi'_m$, and taking into account that $\nabla_T^2 \psi_r^{(p)} = -\kappa_r^{(p)2} \psi_r^{(p)}$, we have

$$\begin{aligned} \int_{S_p} \vec{e}_r^{(p)} \cdot \vec{\mathcal{E}}'_m dS &= \frac{1}{\kappa_r^{(p)} k'_m} \int_{\partial S_p} \chi'_m \vec{n}_p \cdot \nabla_T \psi_r^{(p)} dl \\ &+ \frac{1}{\kappa_r^{(p)} k'_m} \int_{\overline{\partial S_p}} \chi'_m \vec{n}_p \cdot \nabla_T \psi_r^{(p)} dl \\ &+ \frac{\kappa_r^{(p)}}{k'_m} \int_{S_p} \psi_r^{(p)} \chi'_m dS \end{aligned} \quad (\text{A.7})$$

By remembering that $\partial \psi_r^{(p)} / \partial n_p = 0$ on ∂S_p and that $\chi'_m = 0$ on $\overline{\partial S_p}$, the line integrals in (A.7) vanish. Therefore, by substituting the surface integral in the r.h.s. of (A.6) into (A.7), and considering $\kappa_r^{(p)2} \neq k_m'^2$, we finally obtain (21).

Derivation of (22)

From (12) and (3) we have

$$\begin{aligned} \int_{S_p} \vec{e}_r^{0(p)} \cdot \vec{\mathcal{E}}'_m dS &= \int_{S_p} \vec{u}_z \times \nabla_T \psi_r^{0(p)} \cdot \frac{\nabla_T \chi'_m}{k'_m} dS \\ &= \frac{1}{k'_m} \int_{S_p} \nabla_T \psi_r^{0(p)} \cdot \nabla_T \chi'_m \times \vec{u}_z dS \quad (\text{A.8}) \end{aligned}$$

By applying (A.1) to (A.8) with $\vec{\mathcal{A}} = \nabla_T \chi'_m \times \vec{u}_z$ and $\mathcal{B} = \psi_r^{0(p)}$, we have

$$\begin{aligned} \int_{S_p} \vec{e}_r^{0(p)} \cdot \vec{\mathcal{E}}'_m dS &= \frac{1}{k'_m} \int_{\partial S_p} \psi_r^{0(p)} \vec{n}_p \cdot \nabla_T \chi'_m \times \vec{u}_z d\ell \\ &+ \frac{1}{k'_m} \int_{\partial S_p} \psi_r^{0(p)} \vec{n}_p \cdot \nabla_T \chi'_m \times \vec{u}_z d\ell \\ &- \frac{1}{k'_m} \int_{S_p} \psi_r^{0(p)} \nabla_T \cdot (\nabla_T \chi'_m \times \vec{u}_z) dS \quad (\text{A.9}) \end{aligned}$$

In the r.h.s. of (A.9), the surface integral vanishes due to (A.4). With regards to the line integral on ∂S_p , $\psi_r^{0(p)} = \text{cost}$ on each contour ∂S_p^i . In the case of a closed contour ∂S_p^i

$$\int_{\partial S_p^i} \vec{n}_p \cdot \nabla_T \chi'_m \times \vec{u}_z d\ell = \int_{\partial S_p^i} \nabla_T \chi'_m \cdot \vec{t}_p d\ell = 0 \quad (\text{A.10})$$

(see [23], Appendix 2, Eq. 55). In the case of an open line ∂S_p^i (only for patches attached to ports),

$$\int_{\partial S_p^i} \vec{n}_p \cdot \nabla_T \chi'_m \times \vec{u}_z d\ell = \int_{\partial S_p^i} \nabla_T \chi'_m \cdot \vec{t}_p d\ell = \chi'_m(P) - \chi'_m(Q) \quad (\text{A.11})$$

where P and Q are extreme points of the line ∂S_p^i , which are located on the box wall ∂S_{box} , where $\chi'_m = 0$. Finally, the line integral on $\overline{\partial S_p}$ vanishes since $\vec{n}_p \cdot \nabla_T \chi'_m \times \vec{u}_z = \partial \chi'_m / \partial t_p = 0$ on $\overline{\partial S_p}$. This proves (22).

Derivation of (23)

From (8) and (4) we have

$$\begin{aligned} \int_{S_p} \vec{e}_r^{i(p)} \cdot \vec{\mathcal{E}}''_m dS &= \int_{S_p} \left(\vec{u}_z \times \frac{\nabla_T \psi_r^{i(p)}}{\kappa_r^{i(p)}} \right) \cdot \left(\frac{\nabla_T \chi''_m}{k''_m} \times \vec{u}_z \right) dS \\ &= -\frac{1}{\kappa_r^{i(p)} k''_m} \int_{S_p} \nabla_T \psi_r^{i(p)} \cdot \nabla_T \chi''_m dS \quad (\text{A.12}) \end{aligned}$$

Therefore, the derivation of (23) is similar to the one of (21), only taking into account the different boundary condition of the scalar potential $\psi_r^{i(p)}$.

Derivation of (24)

From (9) and (4) we have

$$\begin{aligned} \int_{S_p} \vec{e}_r^{ii(p)} \cdot \vec{\mathcal{E}}''_m dS &= \int_{S_p} \frac{\nabla_T \psi_r^{ii(p)}}{\kappa_r^{ii(p)}} \cdot \left(\frac{\nabla_T \chi''_m}{k''_m} \times \vec{u}_z \right) dS \\ &= \frac{1}{\kappa_r^{ii(p)} k''_m} \int_{S_p} \nabla_T \psi_r^{ii(p)} \cdot \nabla_T \chi''_m \times \vec{u}_z dS \quad (\text{A.13}) \end{aligned}$$

By applying (A.1) to (A.13) with $\vec{\mathcal{A}} = \nabla_T \chi''_m \times \vec{u}_z$ and $\mathcal{B} = \psi_r^{ii(p)}$, we have

$$\begin{aligned} \int_{S_p} \vec{e}_r^{ii(p)} \cdot \vec{\mathcal{E}}''_m dS &= \frac{1}{\kappa_r^{ii(p)} k''_m} \int_{\partial S_p} \psi_r^{ii(p)} \vec{n}_p \cdot \nabla_T \chi''_m \times \vec{u}_z d\ell \\ &+ \frac{1}{\kappa_r^{ii(p)} k''_m} \int_{\partial S_p} \psi_r^{ii(p)} \vec{n}_p \cdot \nabla_T \chi''_m \times \vec{u}_z d\ell \\ &- \frac{1}{\kappa_r^{ii(p)} k''_m} \int_{S_p} \psi_r^{ii(p)} \nabla_T \cdot (\nabla_T \chi''_m \times \vec{u}_z) dS \quad (\text{A.14}) \end{aligned}$$

In the r.h.s. of (A.14), the surface integral vanishes due to (A.4). In the case of patches connected to ports, the line integral on $\overline{\partial S_p}$ vanishes since $\psi_r^{ii(p)} = 0$ on $\overline{\partial S_p}$. Moreover, in the line integral ∂S_p , $\vec{n}_p \cdot \nabla_T \chi''_m \times \vec{u}_z = \nabla_T \chi''_m \cdot \vec{t}_p$. This proves (24).

Derivation of (25)

From (12) and (4) we have

$$\begin{aligned} \int_{S_p} \vec{e}_r^{0(p)} \cdot \vec{\mathcal{E}}''_m dS &= \\ &\int_{S_p} \left(\vec{u}_z \times \nabla_T \psi_r^{0(p)} \right) \cdot \left(\frac{\nabla_T \chi''_m}{k''_m} \times \vec{u}_z \right) dS \\ &= -\frac{1}{k''_m} \int_{S_p} \nabla_T \psi_r^{0(p)} \cdot \nabla_T \chi''_m dS \quad (\text{A.15}) \end{aligned}$$

By applying (A.1) to (A.15) with $\vec{\mathcal{A}} = \nabla_T \psi_r^{0(p)}$ and $\mathcal{B} = \chi''_m$, we have

$$\begin{aligned} \int_{S_p} \vec{e}_r^{0(p)} \cdot \vec{\mathcal{E}}''_m dS &= \frac{1}{k''_m} \int_{\partial S_p} \chi''_m \vec{n}_p \cdot \nabla_T \psi_r^{0(p)} d\ell \\ &+ \frac{1}{k''_m} \int_{\partial S_p} \chi''_m \vec{n}_p \cdot \nabla_T \psi_r^{0(p)} d\ell \\ &- \frac{1}{k''_m} \int_{S_p} \chi''_m \nabla_T^2 \psi_r^{0(p)} dS \quad (\text{A.16}) \end{aligned}$$

In the r.h.s. of (A.16), the surface integral vanishes because $\nabla_T^2 \psi_r^{0(p)} = 0$, whereas the line integral on $\overline{\partial S_p}$ vanishes since $\partial \psi_r^{0(p)} / \partial n_p = 0$ on $\overline{\partial S_p}$. This proves (25).

REFERENCES

- [1] T. Ishikawa, E. Yamashita, "Experimental Evaluation of Basic Circuit Components Using Buried Microstrip Lines for Constructing High-Density Microwave Integrated Circuits," *IEEE Trans. Microwave Theory Tech.*, Vol. MTT-44, No. 7, pp. 1074–1080, July 1996.
- [2] H. Okazaki, T. Hirota, "Multilayer MMIC Broad-Side Coupler with a Symmetric Structure," *IEEE Microwave and Guided Wave Lett.*, Vol. 7, No. 6, pp. 145–146, June 1997.
- [3] J.-S. Hong, M.J. Lancaster, "Aperture-Coupled Microstrip Open-Loop Resonators and Their Applications to the Design of Novel Microstrip Bandpass Filters," *IEEE Trans. Microwave Theory Tech.*, Vol. MTT-47, No. 9, pp. 1848–1855, Sept. 1999.
- [4] J.-Y. Lee, T.-S. Horng, N.G. Alexopoulos, "Analysis of Cavity-Backed Aperture Antennas with a Dielectric Overlay," *IEEE Trans. Antennas Propag.*, Vol. AP-42, No. 11, pp. 1556–1562, Nov. 1994.
- [5] L.P. Dunleavy, P.B. Katehi, "A Generalized Method for Analyzing Shielded Thin Microstrip Discontinuities," *IEEE Trans. Microwave Theory Tech.* Vol. MTT-36, No. 12, pp. 1758–1766, Dec. 1988.

- [6] G.V. Eleftheriades, J.R. Mosig, M. Guglielmi, "A Fast Integral Equation Technique for Shielded Planar Circuits Defined on Nonuniform Meshes," *IEEE Trans. Microwave Theory Tech.*, Vol. MTT-44, No. 12, pp. 2293-2296, Dec. 1996.
- [7] A. Hill, V.K. Tripathi, "An Efficient Algorithm for the Three-Dimensional Analysis of Passive Microstrip Components and Discontinuities for Microwave and Millimeter-Wave Integrated Circuits," *IEEE Trans. Microwave Theory Tech.* Vol. MTT-39, No. 1, pp. 83-91, Jan. 1991.
- [8] S.M. Rao, D.R. Wilton, A.W. Glisson, "Electromagnetic Scattering by Surfaces of Arbitrary Shape," *IEEE Trans. Antennas Propag.* Vol. AP-30, No. 3, pp. 409-418, May 1982.
- [9] N. Kinayman, M.I. Aksun, "Efficient Use of Closed-Form Green's Functions for the Analysis of Planar Geometries with Vertical Connections," *IEEE Trans. Microwave Theory Tech.* Vol. MTT-45, No. 5, pp. 593-603, May 1997.
- [10] A. Alvarez Melcón, J.R. Mosig, M. Guglielmi, "Efficient CAD of Boxed Microwave Circuits Based on Arbitrary Rectangular Elements," *IEEE Trans. Microwave Theory Tech.*, Vol. MTT-47, No. 7, pp. 1045-1058, July 1999.
- [11] G. Conciauro, M. Guglielmi, R. Sorrentino, *Advanced Modal Analysis*, Chap. 5, John Wiley and Sons, 2000.
- [12] M. Bozzi, L. Perregrini, A. Alvarez Melcon, M. Guglielmi, G. Conciauro, "MoM/BI-RME Analysis of Boxed Microwave Circuits Based on Arbitrarily Shaped Elements," *International Microwave Symposium 2001*, Phoenix, AZ, USA, 20-25 May 2001.
- [13] J.C. Rautio, R.F. Harrington, "An Electromagnetic Time-Harmonic Analysis of Shielded Microstrip Circuits," *IEEE Trans. Microwave Theory Tech.* Vol. MTT-35, No. 8, pp. 726-730, Aug. 1987.
- [14] G.V. Eleftheriades, J.R. Mosig, "On the Network Characterization of Planar Passive Circuits Using the Method of Moments," *IEEE Trans. Microwave Theory Tech.*, Vol. MTT-44, No. 3, pp. 438-445, March 1996.
- [15] L.B. Felsen, N. Marcuvitz, "Radiation and Scattering of Waves," *Prentice-Hall*, New Jersey, USA, 1973.
- [16] G. Conciauro, M. Bressan, "Singularity Expansion of Mode Voltages and Currents in a Layered Anisotropic Dispersive Medium Included Between Two Ground Planes," *IEEE Trans. Microwave Theory Tech.*, Vol. MTT-47, No. 9, pp. 1617-1626, Sept. 1999.
- [17] G. Conciauro, M. Bressan, C. Zuffada, "Waveguide Modes Via an Integral Equation Leading to a Linear Matrix Eigenvalue Problem", *IEEE Trans. Microwave Theory Tech.*, Vol. MTT-32, No. 11, pp. 1495-1504, Nov. 1984.
- [18] G. Conciauro, P. Arcioni, M. Bressan, L. Perregrini, "Wideband Modeling of Arbitrarily Shaped H-Plane Waveguide Components by the 'Boundary Integral-Resonant Mode Expansion Method'," *IEEE Trans. Microwave Theory Tech.*, Vol. MTT-44, No. 7, pp. 1057-1066, July 1996.
- [19] P. Arcioni, M. Bressan, G. Conciauro, L. Perregrini, "Wideband Modeling of Arbitrarily Shaped E-Plane Waveguide Components by the 'Boundary Integral-Resonant Mode Expansion Method'," *IEEE Trans. Microwave Theory Tech.*, Vol. MTT-44, No. 11, pp. 2083-2092, Nov. 1996.
- [20] C.-C. Yu, K. Chang, "Novel Compact Elliptic-Function Narrow-Band Bandpass Filters Using Microstrip Open-Loop Resonators With Coupled and Crossing Lines," *IEEE Trans. Microwave Theory Tech.*, Vol. MTT-46, No. 7, pp. 952-958, July 1998.
- [21] G. G. Gentili, "Properties of TE-TM Mode-Matching Techniques," *IEEE Trans. Microwave Theory Tech.*, Vol. MTT-39, No. 9, pp. 1669-1673, Sept. 1991.
- [22] P. Guillot, P. Couffignal, H. Baudrand, B. Theron, "Improvement in Calculation of Some Surface Integrals: Application to Junction Characterization in Cavity Filter Design," *IEEE Trans. Microwave Theory Tech.*, Vol. MTT-41, No. 12, pp. 2156-2160, Dec. 1993.
- [23] J. Van Bladel, *Electromagnetic Fields*, Hemisphere, Washington, DC, 1985.



Maurizio Bozzi (S'98, M'01) was born in Voghera, Italy, in 1971. He received the "Laurea" degree in Electronic Engineering and the Ph.D. in Electronics and Computer Science from the University of Pavia, Pavia, Italy, in 1996 and 2000, respectively. From December 1996 to September 1997 he was a guest researcher at the Technische Universität Darmstadt, Darmstadt, Germany, in the framework of a European TMR project. Since 1997, he has been with the Department of Electronics, University of Pavia. His main research activities concern the electromagnetic modeling of frequency selective surfaces, quasi-optical frequency multipliers, and microwave printed and integrated circuits. Dr. Bozzi was awarded the MECSA prize for the best paper presented by a young researcher at the 2000 Italian Conference on Electromagnetics (XIII RINEM). He is a member of the Society of Photo-Optical Instrumentation Engineers (SPIE) and a Correspondent of the International Union of Radio Science (URSI). He serves on the Editorial Board of the IEEE TRANSACTIONS ON MICROWAVE THEORY AND TECHNIQUES.

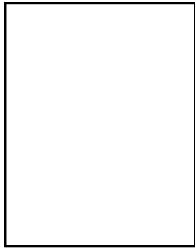


Luca Perregrini (M'98) was born in Sondrio, Italy, in 1964. He graduated in Electronic Engineering and got a Ph.D. in Electronics and Computer Science from the University of Pavia, Italy, in 1989 and 1993, respectively. In 1992, he joined the Department of Electronics of the University of Pavia as an Assistant Professor in electromagnetics and has held a course in Electromagnetic Field Theory since 1996. His current research interests are in numerical methods for the analysis and optimization of waveguide circuits, in the electromagnetic modeling of quasi-optical circuits (frequency multipliers and frequency selective surfaces) in the millimeter and sub-millimeter wave range, and in the modeling of microwave printed and integrated circuits.



Alejandro Alvarez Melcón was born in Madrid, Spain, in 1965. He received the Ingeniero Superior de Telecomunicaciones degree from the Polytechnic University of Madrid (UPM), Madrid, Spain, in 1991, and the Ph.D. degree in electrical engineering from the Swiss Federal Institute of Technology, Lausanne, Switzerland, in 1998. In 1988 he joined the Signal, Systems and Radiocommunications Department, UPM, as a research student, where he was involved in the design, testing, and measurement of broad-band spiral antennas for electromagnetic measurements support (EMS) equipment. From 1991 to 1993, he joined the Radio Frequency Systems Division, European Space Agency (ESA/ESTEC), Noordwijk, The Netherlands, where he was involved in the development of analytical and numerical tools for the study of waveguide discontinuities, planar transmission lines, and microwave filters. From 1993 to 1995, he joined the Space Division, Industry Alcatel Espacio, Madrid, Spain, and he worked at the ESA, where he collaborated in several ESA/ESTEC contracts. From 1995 to 1999, he joined the Swiss Federal Institute of Technology, École Polytechnique Fédérale de Lausanne, Lausanne, Switzerland, where he worked in the field of microstrip antennas and printed circuits for space applications. In 2000, he joined the Polytechnic University of Cartagena, Cartagena, Spain, where he is currently developing his teaching and research activities.

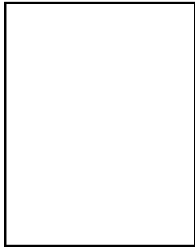
Mr. Alejandro Alvarez Melcón received the JINA Best Paper Award for the best contribution to the JINA'98 International Symposium on Antennas, and the COIT/AEIT Award to the best Ph.D. thesis in basic information and communication technologies.



Marco Guglielmi (SM'98) was born in Rome, Italy, on December 17, 1954. He received the Laurea in Ingegneria Elettronica degree from the University of Rome "La Sapienza, Rome, Italy, in 1979, attended the Scuola di Specializzazione in Elettromagnetismo Applicato in 1980, received the M.S. degree in electrical engineering from the University of Bridgeport, Bridgeport, CT, in 1982, and the Ph.D. degree in electrophysics from Polytechnic University, Brooklyn, NY, in 1986.

From 1984 to 1986, he was an Academic Associate at Polytechnic University. From 1986 to 1988, he was an Assistant Professor at the New Jersey Institute of Technology, Newark, NJ. In 1988, he joined the RF System Division, European Space Research and Technology Center, Noordwijk, The Netherlands, where he is currently involved in the development of passive microwave components for space applications. He is currently with the European Space Research and Technology Center, Noordwijk, The Netherlands. His professional interests include the areas of solid-state devices and circuits, periodic structures, phased arrays, and millimeter-wave leaky-wave antennas, network representations of waveguide discontinuities, and microwave filtering structures.

Dr. Guglielmi was the recipient of a 1981 Fulbright Scholarship in Rome, Italy, and an Halsey International Scholarship Program (HISP) Scholarship from the University of Bridgeport.



Giuseppe Conciauro (A'72, M'87) was born in Palermo, Italy, in 1937. He received the electrical engineering degree and "Libera Docenza" degree from the University of Palermo, Palermo, Italy, in 1961 and 1971, respectively. From 1963 to 1971, he was with the Institute of Electrical Engineering of the University of Palermo, as an Assistant Professor of microwave theory. In 1971 he joined the Department of Electronics, University of Pavia, Pavia, Italy, as an Associate Professor. Since

1980 he has been a Full Professor of electromagnetic theory. From 1985 to 1991, he served as Director of the Department of Electronics.

He authored the textbook *Introduzione alle Onde Elettromagnetiche* (Milano, Italy, McGraw-Hill Italia, 1992) and co-authored *Advanced Modal Analysis* (Chichester, UK, John Wiley and Sons, 2000). His main research interests are in microwave theory, interaction structures for particle accelerators, and numerical methods in electromagnetics.

Prof. Conciauro serves on the Editorial Board of the IEEE TRANSACTIONS ON MICROWAVE THEORY AND TECHNIQUES.